

NUMERICAL SOLUTION OF MHD CONVECTIVE IMMISCIBLE MICROPOLAR AND VISCOUS FLUID FLOW IN A VERTICAL CHANNEL WITH VELOCITY SLIP

Vasavi Cheruku^{1,*}, B Ravindra Reddy²

¹ Department of Mathematics, Sreyas Institute of Engineering and Technology, Hyderabad, Telangana

² Department of Mathematics, JNTUH College of Engineering Hyderabad, Hyderabad, 500085, India.

Abstract

The present paper deals with Numerical analysis for a coupled nonlinear system of partial differential equations governed by immiscible micropolar and viscous fluid flow in a vertical channel when velocity slip is placed on the left wall subjected to the suitable boundary and interface conditions using Runge-Kutta 6th order with Mathematica application. The variation of pertinent parameters is analyzed on velocity, angular velocity, temperature, and diffusion profiles and presented graphically for easy understanding. The rate of velocity transfer, rate of heat transfer, and rate of mass transfer are tabulated for all the possible variations of governing parameters. It is found that the velocity slip has shown a major effect on velocity, angular velocity, and diffusion. Also, there is a reasonable effect on the transfer rate on both boundaries.

Keywords: Vertical channel, micropolar fluid, velocity slip, R-K Method

1. INTRODUCTION

The study of fluid dynamics is the motion and rest of liquids, gases, blood, and plasmas. There are several applications of fluid mechanics in astronomy, mechanical and chemical engineering, and biological systems [1]. Many different branches of science, engineering, and technology deal with the two-phase flow on regular basis. Oil and gas production, gas-liquid flow in boilers, and aerosol deposition in spray treatment are just a few examples of the remarkable benefits of two-phase flows. Inkjets, clouds, fog, groundwater flow, ocean waves, and pest management, among other things, all exhibit two-phase flows. Several researchers [2-5] examined two-phase flows in different geometries.

Lou et al.[6] used the lattice Boltzmann technique to investigate a steady two-phase flow in very narrow channels. Chalgeri and Jeong[7] investigated two-phase flows in a channel with rectangular walls experimentally. The fluid and particle combination is referred to as particulate flows. Usha et al.[8] studied particle suspension flow in an uneven channel numerically. Chamka and Al-Rashidi [9] performed analytical studies on the flow of hydromagnetic particle suspensions over a channel. Yao et al. [10] convincingly illustrated how fluid and particles travel through a conduit by taking slip effects into consideration. Hatami et al. [11] studied the effects of a magnetic field on the two-phase flow between two parallel plates. Kamel et al. [12] investigated the transport of a fluid-particle suspension in a tube with flexible walls by taking slip effects along the wall into account. Eldesoky et al. [13] investigated particle suspension in a tube with undulating walls analytically. Kalpana et al. [14]

used the finite difference method to investigate the buoyancy-driven dusty nanofluids along a non-uniform surface. Dusty free convection Siddiqua et al. [15] investigated Casson fluid using a truncated cone analysis. They discovered that when the thermal radiation parameter rises, the amount of heat transmission increases as well.

The study of MHD has become one of the important subjects, the extensive use of MHD in accelerators, cooling systems with liquid metals, geothermal energy extraction, compacted beds for the chemical industry, MHD power generators, plasma studies, boundary layer control in the field of aerodynamics etc. Asadulla et al. [16] studied hydromagnetic flow in channels with irregular walls. To analyze flow through non-uniform channels under the influence of the magnetic field, Hosseini et al. [17] used the differential transform approach. To examine nanofluid flow analysis in permeable walled channels with the influence of the magnetic field, Hatami and Ganji [18] utilized the weighted residual approach. The heat transfer analysis in communicative channels with non-parallel walls was studied by Erdinc and Yilmaz [19], who found that the heat transfer rate in convergent and divergent channels is much higher than that in channels with parallel walls.

Micropolar fluid is a type of liquid that exhibits specific microscopic effects arising from the regional structure and micro motion of the fluid particles Eringen [20-21]. Bhargava et al. [22] studied that, free convection magnetic hydrodynamics micropolar fluid between two porous vertical plates shows that the velocity decreases with an increase in Hartman number. Airman et al. [23] described the detailed review problem of the matter and its application to the unique characteristics of micropolar fluid mechanics. Micropolar fluids are applicable in the lubrication theory [24], and granular flows [25,26]. The heat transfer process known as thermal radiation involves releasing internal energy. Thermal energy is transformed into electromagnetic energy. Industries like glass manufacturing, polymer manufacturing, and furnace design demonstrate its applicability. processing tech., nuclear power plants, etc. Gerdrood-Bary et al. [27] conducted a numerical examination of thermal radiation's effects on convergent and divergent channels and discovered that the fluid temperature rose along with the radiation parameter. The impact of thermal radiation in non-uniform channels was studied by Asadullah et al. [28] using the A domain decomposition approach. Rashad et al [29] are a numerical investigation of heat and mass transmission in a revolving cone with a thermal radiation effect. Ahmad et al. [30] analysed numerically Jeffrey fluid in convergent and divergent channels with contracting or expanding walls.

The theory of slip effects is unusual, including fluids not adhering to boundaries. There are many uses for the fluid slip at the boundaries, including polishing heart valves and interior cavities, lowering friction and energy conservation, etc. In their study of the effects of slip conditions in a planar channel, Abumandour et al. [31] found that the velocity increases as the slip parameter increase, but that it decreases at higher values of the compressibility parameter when the slip parameter is increased. Analytical magnetohydrodynamics (MHD) flow of particulate suspension flow of Ree-Eyring fluid in a channel with non-uniform walls was explored by Ijaz et al. [32] who found that the magnitude of velocity reduces under the influence of the Hartmann number. Dorrepaal [33] first examined analytically the effects of slip

circumstances in convergent and divergent channels, finding that the slip conditions increase the channel's flow rate. Mohyud-Din et al. [34] used both analytical and numerical methods to investigate the first order velocity and thermal slip effects of a nanofluid in non-uniform channels. Khan et al. [35]'s investigation looked at the impact of velocity slip on a Casson fluid in divergent and convergent channels. Farooq et al. [36] investigated flow through a non-uniform permeability channel with the impact of the transverse magnetic field using the Adomian method and found that the magnetic field effect is more significant on fluid flow. Saleem et al. [37] in their study of peristaltic flow in a non-uniform channel, took into account the second-order velocity slip to analyze heat and mass transfer. In a channel with flexible walls, Manjunatha et al. [38] investigated how changing characteristics affected Jeffrey's fluid flow. Andersson [39] and Wang [40] studied the viscous fluid flow with the slip velocity effect across a stretched surface. Mahabaleshwar et al. have performed investigations on the boundary layer flow with slip effect employing Newtonian fluid [41,42]. According to Ebaid et al. [43], the slip parameter increased the temperatures of both Cu-water and TiO₂-water nanofluids. The velocity profile was also improved by an increase in the velocity slip parameter, according to Bhattacharya et al. [44] and Aziz et al. [45]. Jusoh et al. [46], Jamaludin et al. [47], and Khashi'ie et al. [48] investigated the effect of velocity slip on the three-dimensional stretching/shrinking flow utilizing nanofluid. In heat and mass transfer numerical solution plays a vital role as it produces different set of values for different combinations of all pertinent parameters. Using these values it can be predicted for what set of values the feasibility occurs.

Based on the above criteria and the importance of velocity slip, the present study is on the numerical solution in an immiscible flow containing both micropolar and viscous fluids in a vertical channel with the effect of velocity slip.

2. MATHEMATICAL FORMULATION

Consider two isothermal parallel plates, divided into two regions and placed at $y = -h_1$ & $y = h_2$. Region-1 is from $-h_1 \leq Y \leq 0$ and is filled with micropolar fluid and region -2 is from $0 \leq Y \leq h_2$ and is filled with viscous fluid. These two regions are maintained at temperatures T_1 & T_2 respectively. Assuming the fluid flow to be one dimensional, laminar, immiscible, incompressible, and constant transport properties with bouncy effect. The fluid motion is assumed to be fully developed and steady. The walls are isothermal with constant concentration and satisfy the relation $T_1 > T_2, C_1 > C_2$.

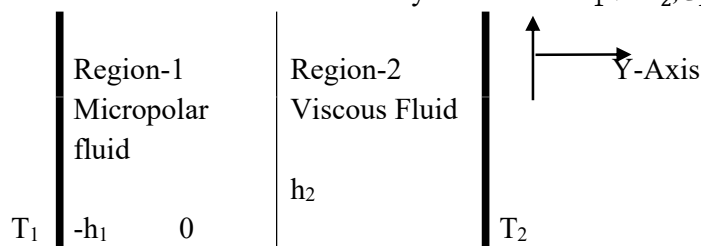


Figure-1: Schematic diagram

The following equations result from the governing equations under the presumptions mentioned above.

Region-1:

$$\frac{\partial U_1}{\partial Y} = 0 \quad (1)$$

$$\rho_1 = \rho_0 [1 - \beta_{1T}(T_1 - T_0) - \beta_{1C}(-C_0)] \quad (2)$$

$$\frac{\mu_1 + K}{\rho_1} \frac{\partial^2 U_1}{\partial Y^2} + \frac{K}{\rho_1} \frac{\partial n}{\partial Y} + g\beta_{1T}(T_1 - T_0) + g\beta_{1C}(C_1 - C_0) - \frac{\sigma B_0^2 U_1}{\rho_1} = 0 \quad (3)$$

$$\gamma \frac{\partial^2 n}{\partial Y^2} - K \left[2n + \frac{\partial U_1}{\partial Y} \right] = 0 \quad (4)$$

$$\text{where } \gamma = \left(\mu_1 + \frac{K}{2} \right) j$$

$$\frac{k_1}{\rho_1 c_p} \frac{\partial^2 T_1}{\partial Y^2} + \frac{1}{\rho_1 c_p} \left[\mu_1 \left(\frac{\partial U_1}{\partial Y} \right)^2 + \frac{\rho_1 D_1 K_{T1}}{c_{S1}} \frac{\partial^2 C_1}{\partial Y^2} \right] = 0 \quad (5)$$

$$D_1 \frac{\partial^2 C_1}{\partial Y^2} + \frac{D_1 K_{T1}}{T_M} \frac{\partial^2 T_1}{\partial Y^2} = 0 \quad (6)$$

Region-2:

$$\frac{\partial U_2}{\partial Y} = 0 \quad (7)$$

$$\rho_2 = \rho_0 [1 - \beta_{2T}(T_2 - T_0) - \beta_{2C}(-C_0)] \quad (8)$$

$$\frac{\mu_2}{\rho_2} \frac{\partial^2 U_2}{\partial Y^2} + g\beta_{2T}(T_2 - T_0) + g\beta_{2C}(C_2 - C_0) - \frac{\sigma B_0^2 U_2}{\rho_2} = 0 \quad (9)$$

$$\frac{k_2}{\rho_2 c_p} \frac{\partial^2 T_2}{\partial Y^2} + \frac{1}{\rho_2 c_p} \left[\mu_2 \left(\frac{\partial U_2}{\partial Y} \right)^2 + \frac{\rho_2 D_2 K_{T2}}{c_{S2}} \frac{\partial^2 C_2}{\partial Y^2} \right] = 0 \quad (10)$$

$$D_2 \frac{\partial^2 C_2}{\partial Y^2} + \frac{D_2 K_{T2}}{T_M} \frac{\partial^2 T_2}{\partial Y^2} = 0 \quad (11)$$

To solve the above system of equations (1) to (11), we considered the following boundary and interface conditions.

$$U_1 = U_0 + S' \frac{\partial U_1}{\partial Y}, \text{ at } Y = -h_1, U_2 = 0, \text{ at } Y = h_2, U_1(0) = U_2(0)$$

$$T = T_1 \text{ at } Y = -h_1, T = T_2, \text{ at } Y = h_2, T_1(0) = T_2(0),$$

$$C = C_1 \text{ at } Y = -h_1, C = C_2, \text{ at } Y = h_2, C_1(0) = C_2(0),$$

$$n = 0 \text{ at } Y = -h_1, (\mu_1 + K) \frac{\partial U_1}{\partial Y} + Kn = \mu_2 \frac{\partial U_2}{\partial Y} \text{ at } Y = 0,$$

$$\frac{\partial n}{\partial Y} = 0 \text{ at } Y = 0, k_1 \frac{\partial T_1}{\partial Y} = k_2 \frac{\partial T_2}{\partial Y} \text{ at } Y = 0, D_1 \frac{\partial C_1}{\partial Y} = D_2 \frac{\partial C_2}{\partial Y} \text{ at } Y = 0.$$

The system of equations (1) to (11) is transformed into a dimensionless form using the following non-dimensional variables:

$$y = \frac{Y}{h_1} (\text{region-1}), y = \frac{Y}{h_2} (\text{region-2}), u_1 = \frac{U_1}{U_0}, u_2 = \frac{U_2}{U_0}, \theta_1 = \frac{T_1 - T_0}{\Delta T}, S = \frac{S'}{h_1}$$

$$C_S = \frac{c_{S1}}{c_{S2}}, K_T = \frac{K_{T1}}{K_{T2}}, D = \frac{D_1}{D_2}, h = \frac{h_1}{h_2}, m = \frac{\mu_1}{\mu_2}, \alpha = \frac{k_1}{k_2}, \rho = \frac{\rho_1}{\rho_2}, b_1 = \frac{\beta_{1T}}{\beta_{2T}}, b_2 = \frac{\beta_{1C}}{\beta_{2C}}, \nu = \frac{\nu_1}{\nu_2}.$$

The following are the dimensionless representations of the governing equations:

Region-1:

$$\frac{\partial^2 N}{\partial y^2} - \frac{2K'}{2+K'} \left(2N + \frac{\partial u_1}{\partial y} \right) = 0 \quad (12)$$

$$(1 + K') \frac{\partial^2 u_1}{\partial y^2} + K' \frac{\partial N}{\partial y} + \frac{Gr}{R} \theta_1 + \frac{Gc}{R} c_1 - Mu_1 = 0 \quad (13)$$

$$\frac{1}{PrPrR} \frac{\partial^2 \theta_1}{\partial y^2} + \frac{Ec}{R} \left(\frac{\partial u_1}{\partial y} \right)^2 + \frac{Du}{R} \frac{\partial^2 c_1}{\partial y^2} = 0 \quad (14)$$

$$\frac{1}{ScR} \frac{\partial^2 c_1}{\partial y^2} + Sr \frac{\partial^2 \theta_1}{\partial y^2} = 0 \quad (15)$$

Region -2

$$\frac{\partial^2 u_2}{\partial y^2} + \frac{m}{b_1 \rho h^2} \frac{Gr}{R} \theta_2 + \frac{m}{b_2 \rho h^2} \frac{Gc}{R} c_2 - \frac{mM}{h^2} u_2 = 0 \quad (16)$$

$$\frac{\rho h}{\alpha} \frac{1}{PrPrR} \frac{\partial^2 \theta_2}{\partial y^2} + \frac{\rho h}{m} \frac{Ec}{R} \left(\frac{\partial u_2}{\partial y} \right)^2 + \frac{c_s h}{DK_T} \frac{Du}{R} \frac{\partial^2 c_2}{\partial y^2} = 0 \quad (17)$$

$$\frac{h}{D} \left(\frac{1}{ScR} \right) \frac{\partial^2 c_2}{\partial y^2} + \frac{h}{K_T D} Sr \frac{\partial^2 \theta_2}{\partial y^2} = 0 \quad (18)$$

The dimensionless boundary and interface conditions thus formed are:

$$u_1 = 1 + s \frac{\partial u}{\partial y} aty = -1, u_2 = 0 aty = 1, u_1(0) = u_2(0),$$

$$\theta_1 = 1 aty = -1, \theta_2 = 0 aty = 1, \theta_1(0) = \theta_2(0),$$

$$c_1 = 1 aty = -1, c_2 = 0 aty = 1, c_1(0) = c_2(0),$$

$$N = 0 aty = -1,$$

$$\frac{\partial u_1}{\partial y} + \frac{K'}{1+K'} N = \frac{1}{mh(1+K')} \frac{\partial u_2}{\partial y} aty = 0,$$

$$\frac{\partial N}{\partial y} = 0 aty = 0, \frac{\partial \theta_1}{\partial y} = \frac{1}{h\alpha} \frac{\partial \theta_2}{\partial y} aty = 0,$$

$$\frac{\partial c_1}{\partial y} = \frac{1}{hD} \frac{\partial c_2}{\partial y} aty = 0. \quad (19)$$

3. SOLUTION OF THE PROBLEM

The system of Non linear equations are solved numerically using Runge-Kutta 6th order method. Numerical calculations have been carried out for different values of governing parameters such as Thermal Grashof number (Gr), Molecular Grashof number (Gc), Reynolds number (R), Magnetic field parameter (M), Material parameter (K'), Dufour number (Du), Schmidt number (Sc), Soret number (Sr) and Eckert number (Ec). The effect governing parameters dimensionless parameters velocity, temperature, concentration are obtained and represented graphically.

4. RESULTS AND DISCUSSIONS

Fig-2 to Fig-7 exhibit the effect of Grashof numbers (Gr) and Molecular grashoff number (Gc) on velocity and angular momentum profiles. It is observed that as Gr increases velocity and angular momentum increases substantially. The fluid velocity increases due to the enhancement of thermal and species buoyancy forces. The effect of Grashof numbers leads to rise in temperature as there is an increment in Gr duo to change in buoyancy. Fig-5 depicts the effect of Grashof numbers (Gr) on Diffusion, slight enhancement in diffusion is recorded as Gr increases. Fig-6 describes the effect of Gc on velocity, due to the enhancement of Bouncy forces velocity increases. Fig-7 reports the effect of Gc on Diffusion. There is a slight increment in diffusion parameter with respect to Molecular Grashof number (Gc).

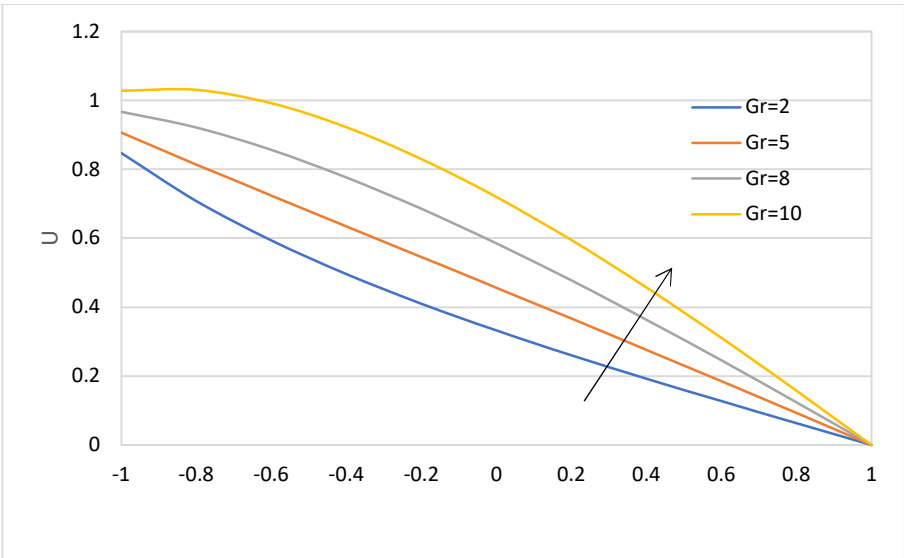


Fig-2: Variation of velocity with Gr

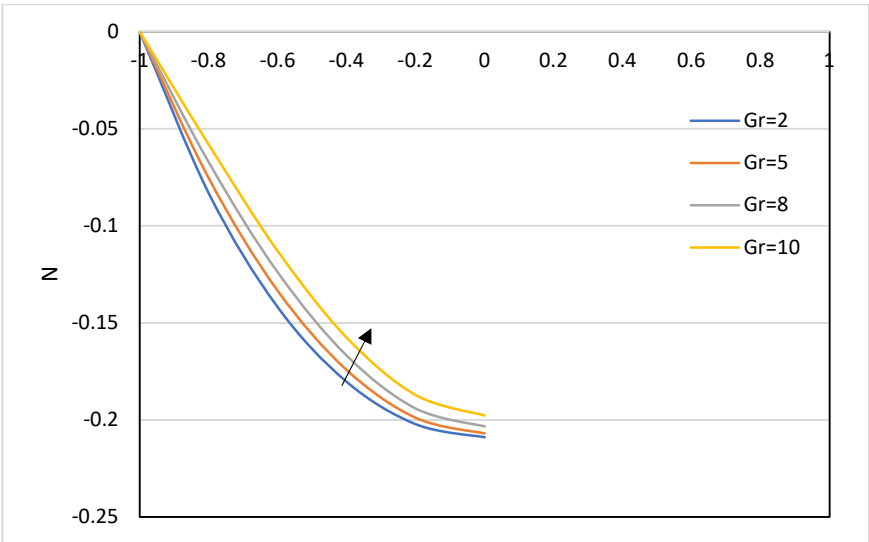


Fig-3: Variation of angular momentum with Gr

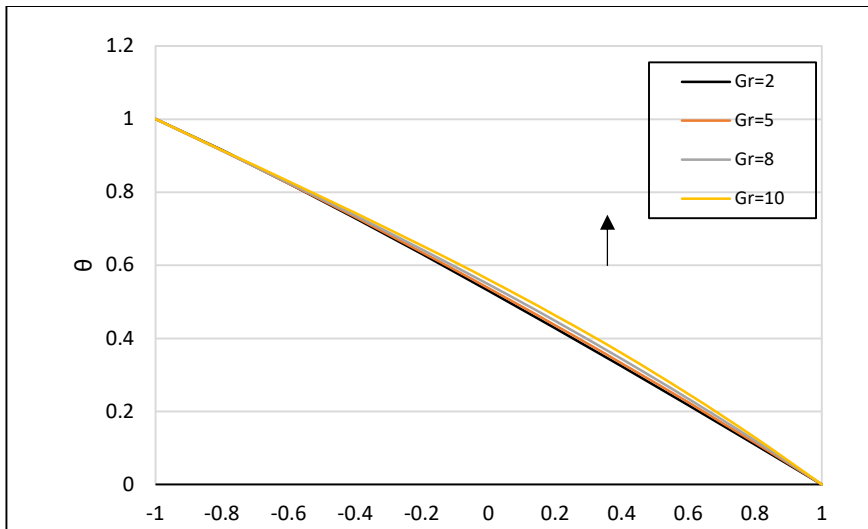


Fig-4: Variation of Temperature with Gr

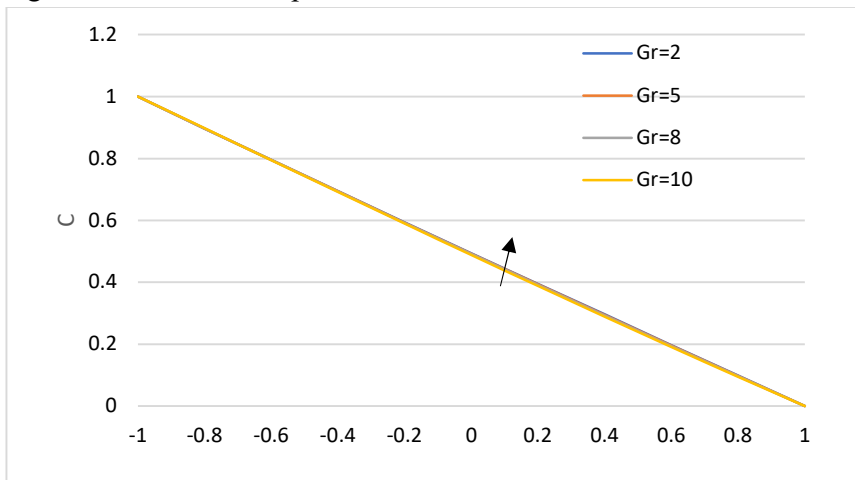


Fig-5: Variation of Diffusion with Gr

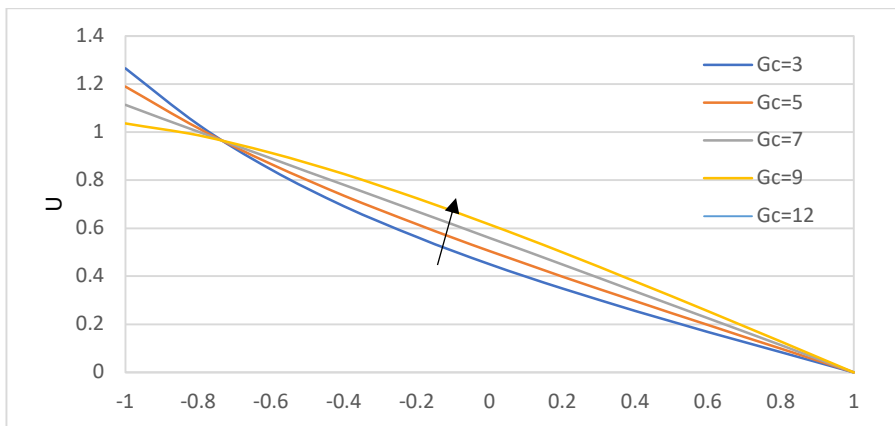


Fig-6: Variation of Velocity with Gc

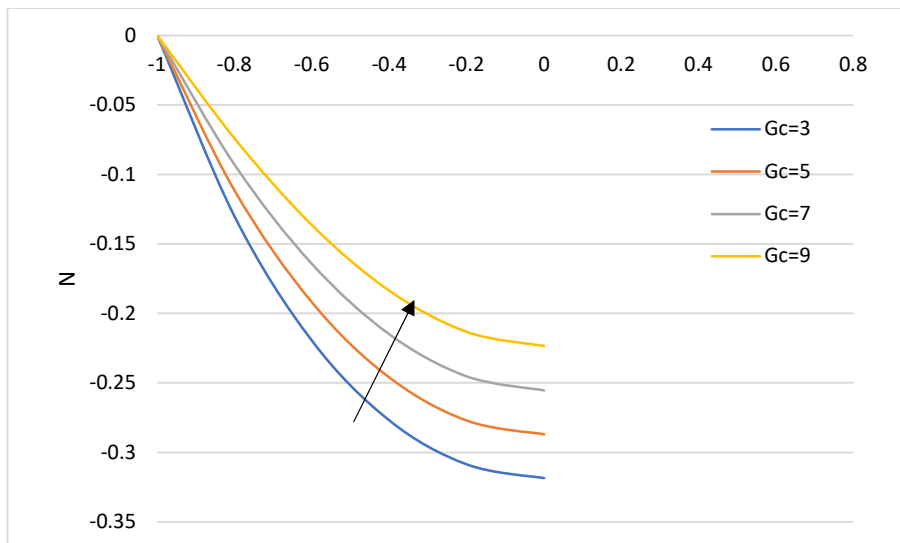


Fig-7: Variation of angular momentum with G_c

Fig-8 to Fig-9 illustrates the influence of micro polar parameter, effect on the velocity and diffusion parameter. It is observed that velocity decreases with increase of K' values. It is significant to note that applying a transverse magnetic field acts as a resistive force (Lorentz force) that acts in the opposite direction of fluid motion and resists flow, hence slowing the velocity of the fluid. As the permeability parameter K' increases, it is seen that the velocity profile decreases. Reverse effect is observed in diffusion. Fig-10 and Fig-12 describes the effect of radiation parameter R on velocity and angular velocity. An increase in R leads to decreasing the velocity and angular velocity. This is due to the fact that high values of R result in a higher conduction-over- R dominance, which reduces the buoyancy thickness of the momentum boundary layer. Fig-11 depicts the effect of Reynolds number R on temperature. It is observed that there is an enhancement in temperature as R increases. Fig-13 illustrates the effects of R on diffusion. There is a reduction in diffusion as R increases.

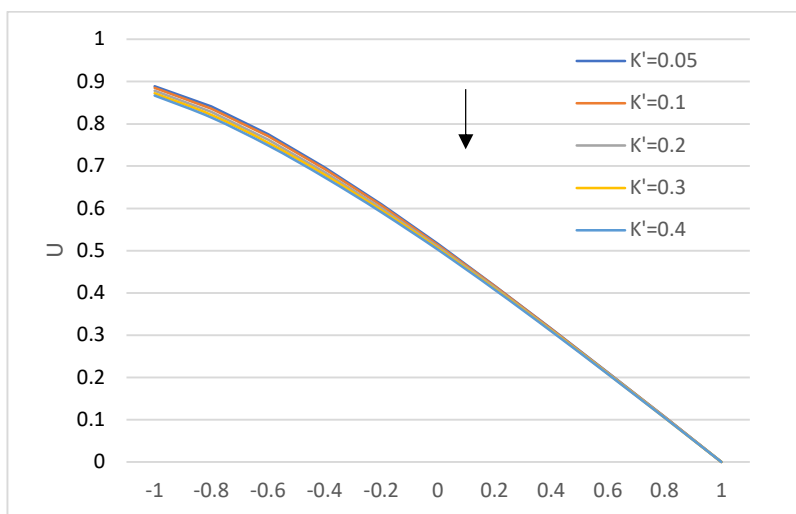


Fig-8: Variation of Velocity with K'

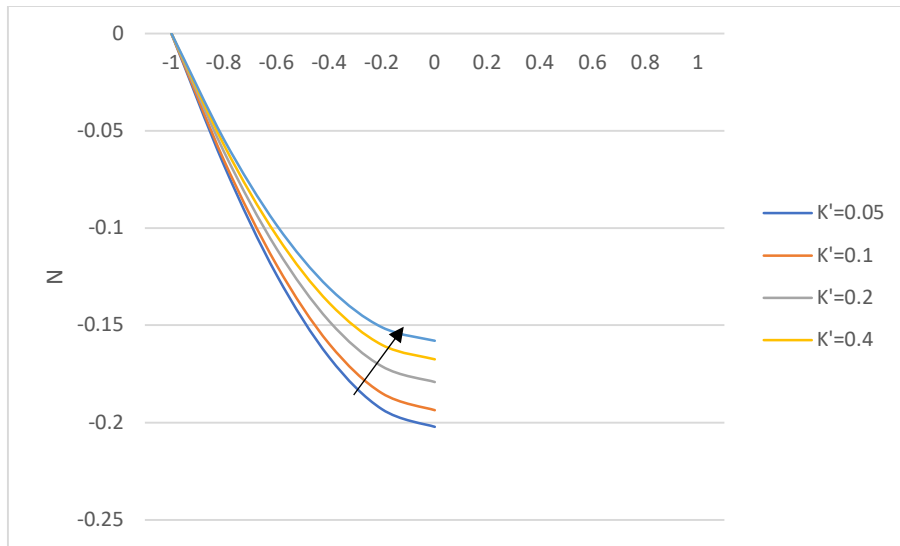


Fig-9: Variation of Diffusion with K'

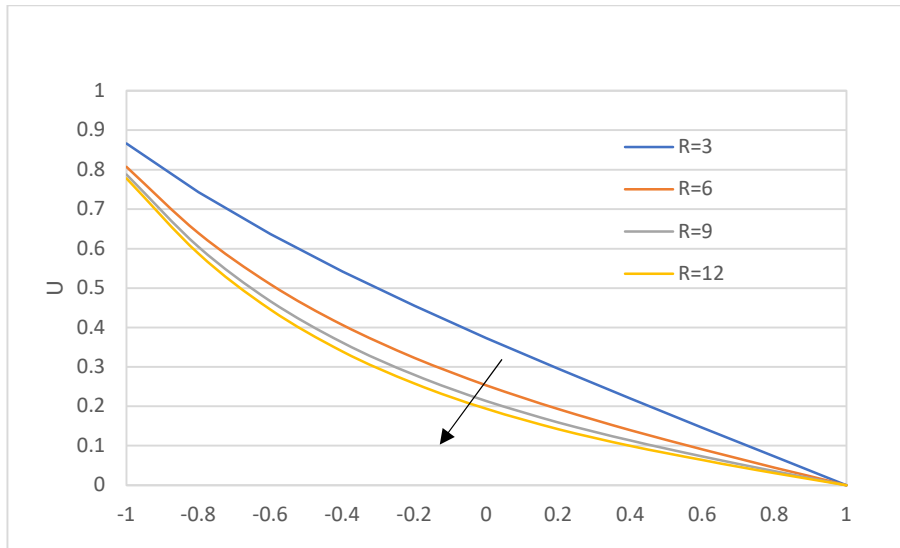


Fig-10: Variation of Velocity with R

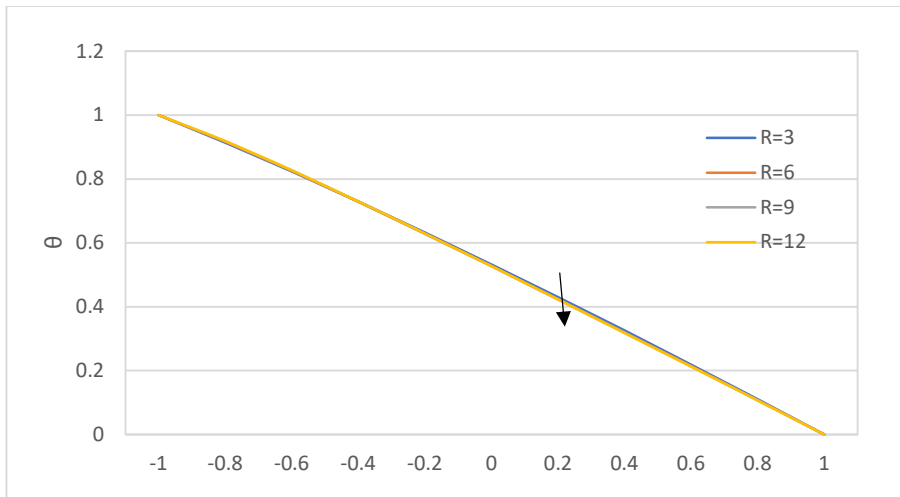


Fig-11: Variation of Temperature with R

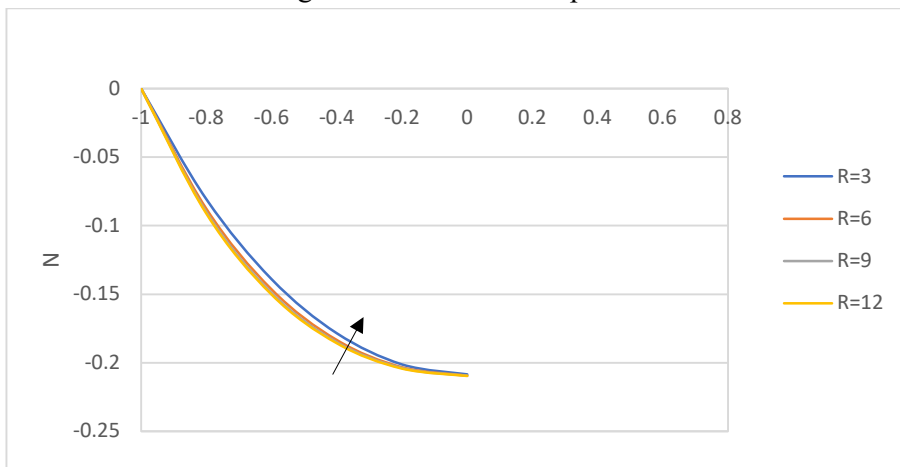


Fig-12: Variation of angular momentum with R

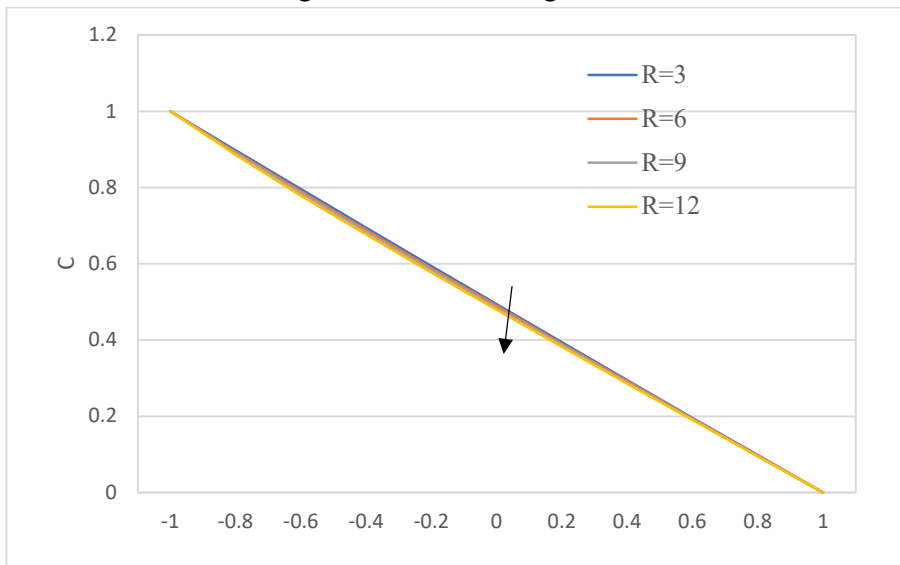


Fig-13 Variation of Diffusion with R

As crux of the work is studying the impact of slip parameter. Many possible values for this are considered when s (velocity slip) is varying as $s = -1.2, -0.9, -0.6, 0, 0.3, 0.6, 0.9, 1.2$ there is gradual decay in the velocity which is displayed in Fig-14. Fig-15 and Fig-17 reports the effect of Slip on temperature and diffusion profiles at $s = -1.2, -0.9, -0.6, -0.3, 0, 0.3, 0.6, 0.9, 1.2$. As the slip parameter s is increasing, temperature and diffusion is decreasing. Fig-16 depicts the effect of Slip parameter angular velocity, the effect is observed as similar velocity.

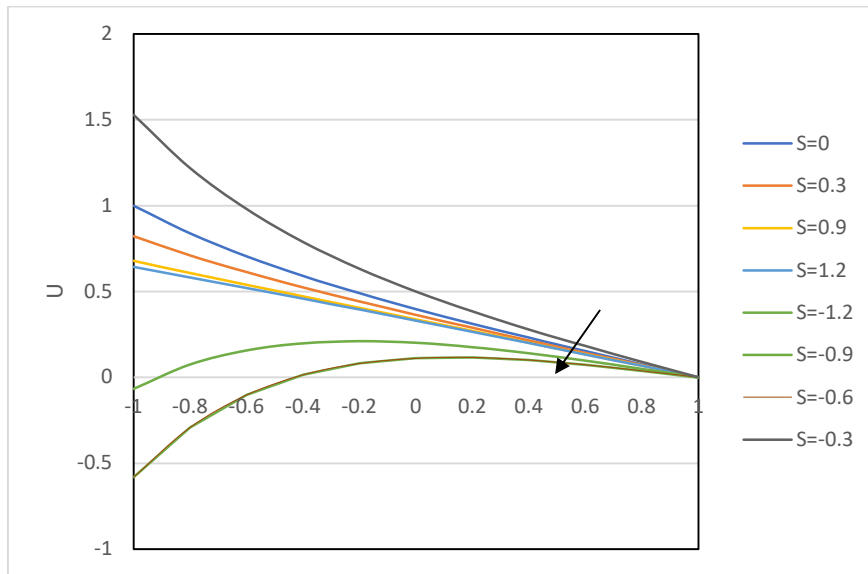


Fig-14: Variation of Velocity with Slip

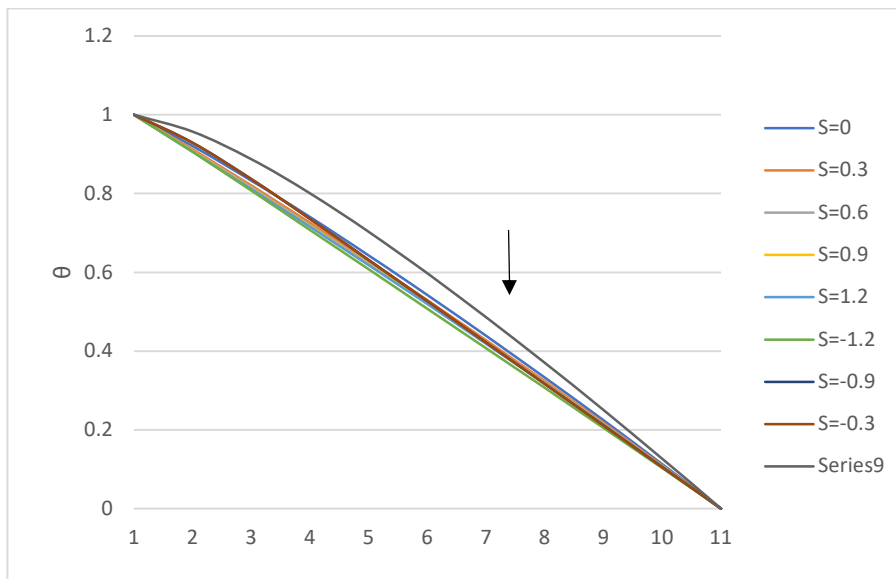


Fig-15: Variation of Temperature with Slip

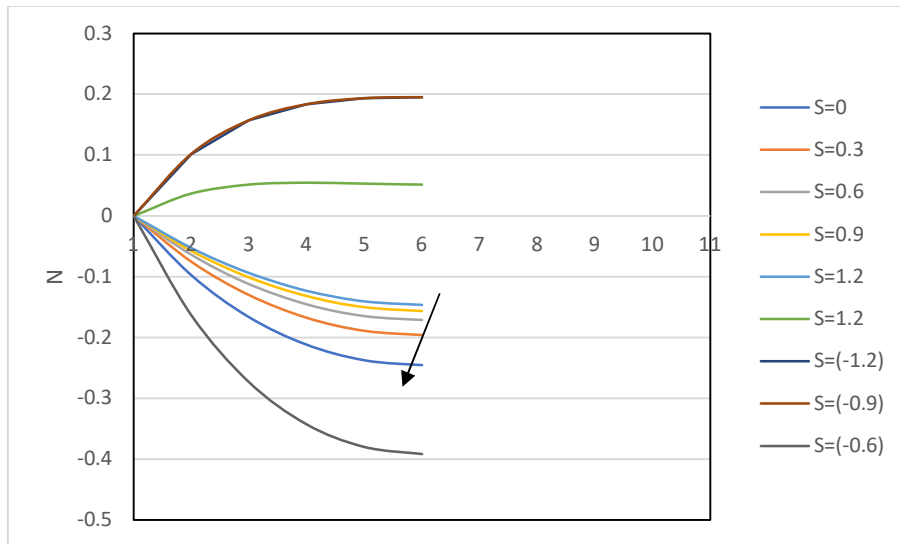


Fig-16: Variation of angular momentum with slip

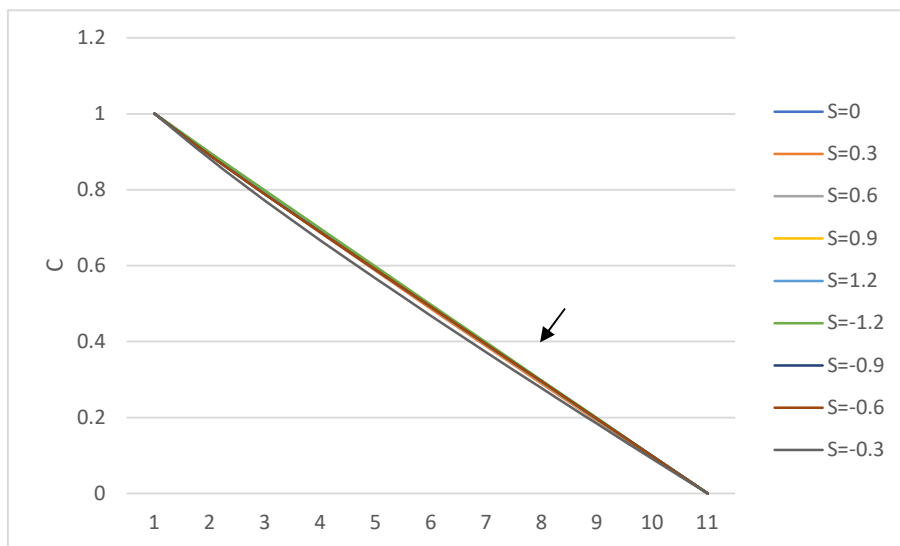


Fig-17: Variation of Diffusion with slip

Gr	$St-I$	$St-II$	$Nu-I$	$Nu-II$	$Sh-I$	$Sh-II$
2	-0.84173	0.2278	0.4908	0.4872	0.6635	0.31451
5	-1.22408	0.357	0.4907	0.4872	0.6635	0.31447
8	-1.60644	0.4862	0.4906	0.4873	0.6635	0.31443
10	-1.86137	0.5723	0.4905	0.4873	0.6636	0.31439
Gc	$St-I$	$St-II$	$Nu-I$	$Nu-II$	$Sh-I$	$Sh-II$
2	-0.87857	0.2654	0.4908	0.4872	0.6635	0.3145
5	-1.22408	0.357	0.4907	0.4872	0.6635	0.31447

8	-1.56958	0.4486	0.4906	0.4872	0.6635	0.31444
10	-1.79991	0.5096	0.4905	0.4873	0.6636	0.31441
<i>R</i>	<i>St-I</i>	<i>St-II</i>	<i>Nu-I</i>	<i>Nu-II</i>	<i>Sh-I</i>	<i>Sh-II</i>
1	-3.76511	1.2101	0.5003	0.4767	0.5453	0.43269
2	-1.85976	0.5707	0.4961	0.4816	0.6033	0.37467
3	-1.22408	0.357	0.4907	0.4872	0.6635	0.31447
5	-0.71423	0.1847	0.4788	0.4991	0.7908	0.18721
<i>M</i>	<i>St-I</i>	<i>St-II</i>	<i>Nu-I</i>	<i>Nu-II</i>	<i>Sh-I</i>	<i>Sh-II</i>
1	-1.57481	0.621	0.4905	0.4873	0.6636	0.31438
2	-1.36598	0.4578	0.4906	0.4872	0.6635	0.31444
3	-1.22408	0.357	0.4907	0.4872	0.6635	0.31447
5	-1.03872	0.2413	0.4908	0.4872	0.6635	0.3145
<i>s</i>	<i>St-I</i>	<i>St-II</i>	<i>Nu-I</i>	<i>Nu-II</i>	<i>Sh-I</i>	<i>Sh-II</i>
0	-1.26154	0.3588	0.4907	0.4872	0.6635	0.31447
0.3	-1.22408	0.357	0.4907	0.4872	0.6635	0.31447
0.6	-1.1571	0.3531	0.4907	0.4872	0.6635	0.31448
0.9	-1.09873	0.3491	0.4907	0.4872	0.6635	0.31448
<i>Du</i>	<i>St-I</i>	<i>St-II</i>	<i>Nu-I</i>	<i>Nu-II</i>	<i>Sh-I</i>	<i>Sh-II</i>
0.08	-1.22408	0.357	0.4907	0.4872	0.6635	0.31447
0.1	-1.224	0.3569	0.4912	0.4867	0.6632	0.31475
0.3	-1.22305	0.3559	0.4971	0.4808	0.66	0.31797
0.5	-1.22173	0.3546	0.5053	0.4727	0.6555	0.32239
<i>Sr</i>	<i>St-I</i>	<i>St-II</i>	<i>Nu-I</i>	<i>Nu-II</i>	<i>Sh-I</i>	<i>Sh-II</i>
0.05	-1.25293	0.3864	0.4991	0.4788	0.5739	0.40405
0.08	-1.23581	0.3689	0.4941	0.4838	0.6271	0.35088
0.1	-1.22408	0.357	0.4907	0.4872	0.6635	0.31447
0.13	-1.20599	0.3385	0.4854	0.4925	0.7196	0.25835
<i>Sc</i>	<i>St-I</i>	<i>St-II</i>	<i>Nu-I</i>	<i>Nu-II</i>	<i>Sh-I</i>	<i>Sh-II</i>
0.22	-1.26221	0.3959	0.5018	0.476	0.5451	0.43286
0.66	-1.22408	0.357	0.4907	0.4872	0.6635	0.31447
1.02	-1.19075	0.3229	0.481	0.4969	0.767	0.21101
1.5	-1.14299	0.2742	0.467	0.5109	0.9152	0.06279

Ec	$St-I$	$St-II$	$Nu-I$	$Nu-II$	$Sh-I$	$Sh-II$
0.001	-1.22408	0.357	0.4907	0.4872	0.6635	0.31447
0.002	-1.22409	0.357	0.4905	0.4873	0.6636	0.31441
0.02	-1.22431	0.3571	0.4873	0.4887	0.6644	0.31333
0.05	-1.22467	0.3573	0.482	0.4911	0.6658	0.31151

Table 3.1 Numerical values of shear stress, Nusselt number, Sherwood numbers

[The above values are obtained when the other parameters are fixed as $Gr=5$, $Gc=5$, $R=3$, $M=3$, $K'=0.1$, $Du=0.08$, $Sr=0.1$, $Sc=0.66$, $Ec=0.001$]

Table 1 shows the computed shear stress, Nusselt number, and Sherwood number together with all possible impact on the governing parameters. This table shows that when the buoyancy forces increase close to the borders, there is an increase in the absolute shear stress, which leads to an improvement in shearing outcomes. Shearing stress at the boundary decreases with an increase in the Reynolds number, magnetic field parameter, material parameter, Dufour number, Soret number, and Schmidt number. In the dissipation parameter Ec , the opposite effect is observed.

The Nusselt number, or rate of heat transfer, decreases close to one boundary and increases at the other for the parameters Gr , Gc , R , Sc , and Ec . Significant changes in the Reynolds Number are seen in the rate of heat transfer. The right plate's heat transfer rate is improved by the elevation of the inertial forces, whereas the left plate's is ruined. Reversal of the effect occurs for the parameters M and K' . The relationship between the Nusselt number and the diffusion parameters Du and Sr demonstrates that as Dufour increases, heat transfer to the left plate is enhanced and to the right boundary is reduced. For Sr , it is entirely in opposition.

The Sherwood number, which measures the rate of mass transfer, increases close to the border and decreases at the boundary for the parameters Gr , Gc , R , Sr , Sc , and Ec . Mass transfer increases close to the left border and decreases at the right boundary for the other parameters M , K' , and Du , respectively.

5. CONCLUSIONS

The impact of all governing parameters was investigated and displayed graphically. Some of the salient findings are as follows:

- There is a significance effect of Gr , Gc , R , K' on velocity, angular momentum, temperature and diffusion profiles.
- There is a significant effect of all the parameters on rate of shear stress, rate of heat transfer, rate of mass transfer.
- The velocity slip which is placed on left wall has a significant effect on all profiles.

References

- [1] A.J. Chamkha, S.S. Al-Rashidi, Analytical solutions for hydromagnetic natural convection flow of a particulate suspension through isoflux-isothermal channels in the presence of a heat source or sink, *Energy Convers. Manag.* 51 (4) (2010) 851-858.

-
- [2] A.J. Chamkha, Hydromagnetic two-phase flow in a channel, *Int. J. Eng. Sci.* 33 (1995) 437-446.
- [3] M.Z. Podowski, Multidimensional modeling of two-phase flow and heat transfer, *Int. J. Numer. Methods Heat Fluid Flow* 18 (3/4) (2008) 491-513.
- [4] S.K.R. Cher, S. Kariveti, S. Pushpavanam, Experimental and numerical investigations of two-phase (liquid-liquid) flow behaviour in rectangular microchannels, *Ind. Eng. Chem. Res.* 49 (2010) 893-899.
- [5] E. Gedik, H. Kurt, Z. Recebli, A. Keçebas, Unsteady flow of twophase fluid in circular pipes under applied external magnetic and electrical fields, *Int. J. Therm. Sci.* 53 (2012) 156-165.
- [6] Q. Lou, M. Yang, H.T. Xu, Numerical investigations of gas-liquid two-phase flows in microchannels, *J. Mech. Eng. Sci.* 232 (3) (2018) 466-476.
- [7] V.S. Chalgeri, J.H. Jeong, Flow patterns of vertically upward and downward air-water two-phase flow in a narrow rectangular channel, *Int. J. Heat Mass Tran.* 128 (2019) 934-953.
- [8] R. Usha, S. Senthilkumar, E.G. Tulapurkara, Numerical study of particulate suspension flow through wavy-walled channels, *Int. J. Numer. Methods Fluid.* 51 (2006) 235-259.
- [9] A.J. Chamkha, S.S. Al-Rashidi, Analytical solutions for hydromagnetic natural convection flow of a particulate suspension through isoflux-isothermal channels in the presence of a heat source or sink, *Energy Convers. Manag.* 51 (4) (2010) 851-858.
- [10] J. Yao, K. Tao, Z.Q. Huang, Flow of particulate-fluid suspension in a channel with porous walls, *Transport Porous Media* 98 (2013) 147-172.
- [11] M. Hatami, KhHosseinzadeh, G. Domairry, M.T. Behnamfar, Numerical study of MHD two-phase Couette flow analysis for fluidparticle suspension between moving parallel plates, *J. Taiwan Inst. Chem. Eng.* 45 (2014) 2238-2245.
- [12] M.H. Kamel, I.M. Eldesoky, P.M. Malur, R.M. Bumandown, Slip effects on peristaltic transport of a particle-fluid suspension in a planar channel, *Appl. Bionics Biomechanics* 2015 (2015) 70357.
- [13] I.M. Eldesoky, S.I. Abdelsalam, R.M. Abumandour, M.H. Kamel, K. Vafai, Interaction between compressibility and particulate suspension on peristaltically driven flow in planar channel, *Appl. Math. Mech.* 38 (1) (2017) 137-154.
- [14] [13] G. Kalpana, K.R. Madhura, S.S. Iyengar, M.S. Uma, Numerical investigation on convective flow of two-phase MHD dusty nanofluids over a wavy surface with Brownian motion and thermophoresis effects, *Int. J. Algorithm. Comput. Math.* 5 (2019) 62.
- [15] S. Siddiqa, N. Begum, T. Iftikhar, M. Rafiq, M.A. Hossain, R.S.R. Gorla, Thermal radiation effects on Casson dusty boundary layer fluid flow along an isothermal truncated vertical cone, *Mech. Eng.* 44 (2019) 7833-7842.
- [16] M. Asadullah, U. Khan, N. Ahmed, R. Manzoor, S. Tauseef, MHD flow of a Jeffery fluid in converging and diverging channels, *Int. J. Mod. Math. Sci.* 6 (2) (2013) 92-106.

- [17] R. Hosseini, S. Poozesh, S. Dinarvand, MHD flow of an incompressible viscous fluid through convergent or divergent channels in presence of a high magnetic field, *J. Appl. Math.* (2012) 157067.
- [18] M. Hatami, D.D. Ganji, MHD nanofluid flow analysis in divergent and convergent Channels using WRM's and numerical method, *Int. J. Numer. Methods Heat Fluid Flow* 24 (5) (2014) 911-919.
- [19] M.T. Erdinc, T. Yölmaz, Numerical investigation of flow and heat transfer in communicating converging and diverging channels, *J. Therm. Eng.* 4 (5) (2018) 2318-2332.
- [20] Eringen, A. C. (1966). Theory of micropolar fluids. *Journal of Mathematics and Mechanics*, 1-18.
- [21] Eringen, A. C. (1972). Theory of thermomicrofluids. *Journal of Mathematical analysis and Applications*, 38(2), 480-496.)
- [22] Bhargava R, Kumar L, Takhar HS. Numerical solution of free convection MHD micropolar fluid flow between two parallel porous vertical plates. *Int. J. Eng. Sci.* 2003; 41: 123–136.
- [23] Ariman, T. M. A. N. D., Turk, M. A., & Sylvester, N. D. (1973). Micro continuumfluidmechanics—a review. *International Journal of Engineering Science*, 11(8), 905-930.
- [24] S. Allen, K. Kline, Lubrication theory for micropolar fluids, *J. Appl. Mech.* 83 (1971) 646–649.
- [25] M. Khonsari, D. Brews, On the performance of finite journal bearings lubricated with micropolar fluids, *STLE Tribology Trans.* 32 (1989) 155–160.
- [26] N. Mitarai, H. Hayakawa, H. Nakanishi, Collisional granular flow as a micropolar fluid, *Phys. Rev. Lett.* 88 (2002), 174301
- [27] M.B. Gerdroodbary, M.R. Takami, D.D. Ganji, Investigation of thermal radiation on traditional Jeffery-Hamel flow to stretchable convergent/divergent channels, *Case Stud. Therm. Eng.* 6 (2015) 28-39.
- [28] A.M. Asadullaha, U. Khan, N. Ahmed, S.T. Mohyud-Din, Analytical and numerical investigation of thermal radiation effects on flow of viscous incompressible fluid with stretchable convergent/divergent channels, *J. Mol. Liq.* 224 (Part A) (2016) 768e775. 178 B. Mallikarjuna et al.
- [29] A.M. Rashad, B. Mallikarjuna, A.J. Chamkha, S.H. Raju, Thermophoresis effect on heat and mass transfer from a rotating cone in a porous medium with thermal radiation, *Afr. Mathemat.* 27 (2016) 1409-1424.
- [30] N. Ahmad, A. Abbasi, U. Khan, S.T. Mohyud-Din, Thermal radiation effects on the flow of Jeffrey fluid in converging diverging stretchable walls, *Neural Comput. Appl.* 30 (2018) 2371-2379.
- [31] R.M. Abunmandour, I.M. Eldesoky, F.A. Kroush, Effect of slip conditions and compressibility on the peristaltic flow of particulate suspension in planar channel, *SN Appl. Sci.* 1 (2019) 1305.

- [32] N. Ijaz, M.M. Bhatti, A. Zeeshan, Heat transfer analysis in MHD flow of solid particles in non-Newtonian Ree-Eyring fluid due to peristaltic wave in a channel, *Therm. Sci.* 23 (2017) 155, [HTTP://doi.org/10.2298/TSCI170220155I](http://doi.org/10.2298/TSCI170220155I).
- [33] J.M. Dorrepaal, Slip flow in converging and diverging channels, *J. Eng. Math.* 27 (1993) 343-356.
- [34] S.T. Mohyud-Din, U. Khan, N. Ahmed, W. Sikander, A study of velocity and temperature slip effects on flow of water based nano fluids in converging and diverging channels, *Int. J. Appl. Comput. Math* 1 (2015) 569-587.
- [35] U. Khan, W. Sikander, N. Ahmad, S.T. Mohyud-Din, Effects of velocity slip on MHD flow of a Non-Newtonian fluid in converging and diverging channels, *Int. J. Comp. Mathem.* 2 (2016) 469-483.
- [36] J. Farooq, M. Mushtaq, S. Munir, M. Ramzan, J.D. Chung, U. Farooq, Slip flow through a non-uniform channel under the influence of transverse magnetic field, *Sci. Rep.* 8 (2018) 13137.
- [37] N. Saleem, S. Akram, F. Afzal, E.H. Aly, A. Hussain, Impact of velocity second slip and inclined magnetic field on peristaltic flow coating with Jeffrey fluid in tapered channel, *Coatings* 10 (1) (2020) .
- [38] G. Manjunatha, C. Rajashekhar, H. Vaidya, K.V. Prasad, K. Vajravelu, Impact of heat and mass transfer on the peristaltic mechanism of Jeffery fluid in a non-uniform porous channel with variable viscosity and thermal conductivity, *J. Therm. Anal. Calorim.* 139 (2020) 1213-1228.
- [39] H.I. Andersson, Slip flow past a stretching surface, *Acta Mech.* 158 (1-2) (2002) 121–125.
- [40] C.Y. Wang, Flow due to a stretching boundary with partial slip—an exact solution of the Navier–Stokes equations, *Chem. Eng. Sci.* 57 (17) (2002) 3745–3747.
- [41] U.S. Mahabaleshwar, K.R. Nagaraju, M.A. Sheremet, P.V. Kumar, G. Lorenzini, Effect of Mass Transfer and MHD Induced Navier's Slip Flow Due to a non-Linear Stretching Sheet, *J. Eng. Thermophysics* 28 (4) (2019) 578–590.
- [42] U.S. Mahabaleshwar, K.R. Nagaraju, M.A. Sheremet, D. Baleanu, E. Lorenzini, Mass transpiration on Newtonian flow over a porous stretching/shrinking sheet with slip, *Chinese J. Phys* 63 (2020) 130–137. N.S. Khashi'ie, et al. *Chinese Journal of Physics* 66 (2020) 157–171 170
- [43] A. Ebaid, F. Al Mutairi, S.M. Khaled, Effect of ss slip boundary condition on the flow and heat transfer of Cu-water and TiO₂-water nanofluids in the presence of a magnetic field, *Adv. Math. Phys.* (2014) 538950.
- [44] K. Bhattacharyya, S. Mukhopadhyay, G.C. Layek GC, Slip effects on boundary layer stagnation-point flow and heat transfer towards a shrinking sheet, *Int. J. Heat Mass Transf.* 54 (1-3) (2011) 308–313.
- [45] R. Jusoh, R. Nazar, I. Pop, Three-dimensional flow of a nanofluid over a permeable stretching/shrinking surface with velocity slip: A revised model, *Phys. Fluids* 30 (3) (2018) 033604.

- [46] A. Jamaludin, R. Nazar, I. Pop, Three-Dimensional Magnetohydrodynamic Mixed Convection Flow of Nanofluids over a Nonlinearly Permeable Stretching/ Shrinking Sheet with Velocity and Thermal Slip, *Appl. Sci.* 8 (7) (2018) 1128.
- [47] N.S. Khashi'ie, N.M. Arifin, R. Nazar, E.H. Hafidzuddin, N. Wahi, I. Pop, A Stability Analysis for Magnetohydrodynamics Stagnation Point Flow with Zero Nanoparticles Flux Condition and Anisotropic Slip, *Energies* 12 (7) (2019) 1268.
- [48] H.F. Oztop, E. Abu-Nada, Numerical study of natural convection in partially heated rectangular enclosures filled with nanofluids, *Int. J. Heat Fluid Flow* 29 (5) (2008) 1326–1336.